Agronomy Research **22**(S2), 659–671, 2024
https://doi.org/10.15159/AR.24.007

Adsorbent potential of cocoa pod husk activated charcoal to remove metals from the Ucayali River

R.M. Lozano-Reátegui[1,*], V. Asencios-Tarazona[1], I.O. Ruiz-Yance[1], M.R. Guerrero-Ochoa[1], W. Pinedo-Chambi[1] and M.M. Mendoza-Carlos[2]

[1]National Intercultural University of the Amazon, Faculty of Engineering and Environmental Sciences, Academic Department of Agro Industrial Engineering, Pucallpa, 25000 Ucayali, Peru
[2]National Intercultural University of the Amazon, Faculty of Engineering and Environmental Sciences, Academic Department of Basic Sciences, Pucallpa, 25000 Ucayali, Peru
[*]Correspondence: rlozanor@unia.edu.pe

Received: October 1st, 2023; Accepted: January 12th, 2024; Published: January 26th, 2024

Abstract. The problem of river water contamination due to the presence of dangerous metals for ichthyological flora and fauna and human health has motivated the search for innovative and feasible solutions. Therefore, the production of activated carbon from cocoa pod husks was investigated to eliminate metals present in the Ucayali River. Response surface methodology was used to optimize the manufacturing of the adsorbent and test its effectiveness in removing metals from water using a factorial design of 3^3 and 3^2, with three replicates each. The optimal amount of activated carbon (18.41 g) was obtained from 200 g of fresh cocoa pod husks. It was converted into activated carbon under the following conditions: thermal modification at 100, 150, and 200 °C; activation time of 1.0, 1.5, and 2.0 h; and pyrolysis and activation at 400, 500, and 600 °C. This allowed the elimination by efficient adsorption of 56.8% Fe^{2+}, 68.4% Al^{3+}, 65.9% Cu^{2+}, and 55.5% Zn^{2+} from Ucayali River, thus demonstrating its adsorbent power. The results will make it possible to manufacture filters to decontaminate water containing heavy metals, thus guaranteeing its consumption.

Key words: adsorption, heavy metals, pyrolysis, thermal modification, water pollution.

INTRODUCTION

In most countries, the waters of rivers are effluent dumps, which carry pollutants, including heavy metals, that negatively affect the fish population by accumulating in the muscles, viscera, and other tissues (Adeyeye & Ashaolu, 2022; Akila et al., 2022; Zaghloul et al., 2022). They also affect the health of residents who use drink these waters and can have a carcinogenic effect. Therefore, it is considered a public health problem in Peru (Ccanccapa-Cartagena et al., 2021) and is also a prevalent problem worldwide (Mariana et al., 2021).

The development of cocoa (*Theobroma cacao*) cultivation has been increasing in the Ucayali-Peru region. In 2021, 20,046 t were harvested, and by February 2022, 1,213 t had been accumulated (López & Alva, 2022), of which 70–75% (Cruz et al., 2012) corresponded to the husks; therefore, between 14,032.2 and 15,034.5 t, and 849.1 and 909.8 t of residues, respectively, were left in the field, increasing environmental and landscape pollution.

Decontaminating the waters of the Ucayali-Peru river, due to the presence of metals, is approached from a perspective of reuse of lignocellulose waste from cocoa pod shells, which comprise 43.6% lignin, 34.4% cellulose, and 11.75% hemicellulose (Díaz-Oviedo et al., 2022), making them excellent raw materials for the production of activated carbon (Valdés-Rodríguez et al., 2022) using pyrolysis (Maulina & Iriansyah, 2018). They contribute to the formation of micropores of appropriate diameters, have a greater surface area, and have appropriate functional groups on their surface, making it a potential and efficient adsorbent for contaminant removal (González-García et al., 2013; Mariana et al., 2021).

Pyrolysis shows promise for dealing with agricultural waste by thermochemical conversion at high temperatures in the absence of oxygen (Mariana et al., 2021) into activated carbon, and has many important effects, particularly on its adsorption capacity, because increasing the temperature from 350 to 650 °C leads to a drastic increase in surface area and carbonisation with the loss of functional groups (Choi & Kan, 2019).

For the production of activated carbon, the values of surface area and micro pore volume, which are influenced by the type of raw material and pyrolysis temperature, obtained at 300–500 °C using coconut shell (*Cocos nucifera*) were 13.0 $m^2 g^{-1}$ and 0.021 $cm^3 g^{-1}$ (Solanki & Boyer, 2017), respectively; 120.0 $m^2 g^{-1}$ and 2.43 $cm^3 g^{-1}$, respectively, using palm (*Elaeis guineensis*) activated carbon at 600 °C (Guo et al., 2016); 605.0 $m^2 g^{-1}$ and 0.421 $cm^3 g^{-1}$, respectively, using wheat straw (*Triticum spp*) at 700 °C (Wu et al., 2018); and 904.1 $m^2 g^{-1}$ and 0.506 $cm^3 g^{-1}$, respectively, using grapefruit peel (*Citrus paradisi*) at 600–900 °C (Chen et al., 2017).

The use of activated carbon made from lignocellulose waste to remove metals from water samples has been successfully tested; thus, Cu^{2+} has been removed from wastewater samples using activated carbon from green vegetables (Sabela et al., 2019). The removal of Fe^{2+} from the Nag-India River was achieved using activated carbon from orange (*Citrus sinensis*) peels (Nandeshwar et al., 2016).

Liu et al. (2020) removed Hg^{2+} from wastewater using activated carbon from rice husks (*Oriza sativa*); Yunus et al. (2020) removed Cr^{3+} and Zn^{2+} from mining effluents in the tile and electroplating industries using melon (*Cucumis melo*); and Olaoye et al. (2018) and Prastuti et al. (2019) removed Cu^{2+} and Cr^{6+} from textile wastewater, and Pb^{2+}, Cr^{3+}, and Cd^{2+} ions from wastewater in the cassava (*Manihot esculenta*) industry using banana (*Musa paradisiaca*).

In agroindustrial waste, which is converted into activated carbon, palm kernel (*Elaeis guineensis*) shells (Baby & Hussein, 2020) have excellent activity in removing metals such as Cr^{6+}, Pb^{2+}, Zn^{2+}, and Cr^{2+} from water samples. The use of cocoa (*T. cacao* L.) pod shells converted into an adsorbent has been shown to be effective in removing Pb^{2+} and Cu^{2+} from water samples from a processing plant containing a mixture of metals and from a refinery and petrochemical company (Odubiyi et al., 2012; Sadheesh et al., 2021).

The reported methodologies for manufacturing activated carbon include the use of chemical activators and the limited use of cocoa pod shells as lignocellulose biomass. The metals removed did not include aluminium (Al^{3+}), copper (Cu^{2+}), iron (Fe^{2+}), and zinc (Zn^{2+}), but were oriented towards chromium (Cr^{6+}) and cadmium (Cd^{2+}), which have not been discussed in depth in the literature.

Therefore, if cocoa pod shells are converted by thermochemical activation, followed by carbonisation, and the thermochemical modification time is controlled, activated carbon with excellent adsorbent characteristics to remove heavy metals from the waters of the Ucayali River will be obtained. Therefore, the purpose of this study was to manufacture activated carbon from cocoa pod shells (*T. cacao* L.) and determine its adsorption efficiency and removal of heavy metals in water samples from the Ucayali River, Peru.

MATERIALS AND METHODS

Manufacture of activated carbon by pyrolysis: experimental and statistical design

Activated carbon was obtained, as described by Tsai et al. (2018), with adaptations comprising: reception, selection, weighed (200 g) on Ohaus-PA512 scale, repeatability 0.01 g, cut into pieces, chopped to 5 mm, thermal modification at 100, 150, and, 200 °C for 1.0, 1.5, and 2.0 h, pyrolysis and thermal activation at 400, 500, and, 600 °C, in a muffle furnace (Thermolyne brand Thermo Fisher Scientific, MA, USA; FB1414M, ± 0.5 °C at 1,000 °C) for 1 h, ground to particles of 149 µm (0.149 mm), washed with distilled water until total decolourisation, dried at 150 °C in an oven (Memmert, precision up to 99.9 °C: 0.1/from 100 °C: 0.5) for 1 h, with 6.4% humidity (ASTM, 1997), and packaging in glass jars. Obtaining activated carbon followed a 3^3 factorial design with three repetitions, because it is a widely used technique to optimize activation conditions to minimize the number of experiments and obtain maximum information (Grich et al., 2024). The response surface methodology was used for its optimization because it was a multi-factor experiment, which allowed us to effectively distinguish the degree and difference of the influence of each factor (Aksoy & Sagol, 2016), the variables studied being the thermal modification temperature (X_1), thermal activation time (X_2), and the carbonization temperature (X_3), whose parameters are shown in Table 1.

Table 1. Variables and their levels for the production of activated carbon

Variable	Unit	Code	-1	0	+1
Change temperature	°C	X_1	100	150	200
Activation time	h	X_2	1.0	1.5	2.0
Pyrolysis/activation temperature	°C	X_3	400	500	600

The weight of the activated carbon obtained was considered the response variable, as represented in Eq. 1.

$$Y_1 = B_0 + B_1X_1 + B_2X_2 + B_3X_3 + B_{11}X_1^2 + B_{12}X_1X_2 + B_{13}X_1X_3 + B_{22}X_2^2 + B_{23}X_2X_3 + B_{33}X_3^2 \quad (1)$$

where Y_1 – response variable (amount of activated carbon); B_0 – coefficient of the constant; B_1, B_2, B_3 – linear coefficients; B_{12}, B_{13}, B_{23} – binary interaction coefficients; B_{11}, B_{22}, B_{33} – quadratic coefficients, and X_1, X_2, X_3 – levels of the variables for manufacturing activated carbon.

Evaluation of the adsorbent activity of activated carbon and statistical analysis

Water samples from the Ucayali River were taken 30 m from the shore at the Reloj Público port, using 1 L glass bottles, which were immediately insulated and stored under refrigeration using thermal boxes.

The effectiveness of the adsorbent was evaluated using atomic absorption spectroscopy, as recommended by Sibal & Espino (2018). For this purpose, 250 mL water samples were collected from the Ucayali River, with Fe^{+2}, Al^{+3}, Cu^{+2}, and Zn^{+2} of 1.37, 0.25, 0.041, and 0.011 mg L^{-1}, respectively. Water samples were spiked with 1, 3, or 5 g of washed and dried activated carbon, shaken at 300 rpm for 30, 60, or 90 min, filtered, packed in glass jars, hermetically sealed, coded, and stored under refrigeration. The adsorption of Fe^{+2}, Al^{+3}, Cu^{+2}, and Zn^{+2} on the water samples by activated carbon was measured by atomic absorption using a spectrophotometer (Labtron, model LAAS-A11, precision $\lambda \leq \pm 0.5$ nm), and a calibration curve was made with five concentrations and a reagent blank in the linear range for each element measured. To evaluate the adsorptive effectiveness of activated carbon in the adsorption of metals from water samples from the Ucayali River, a factorial 3^2 design with three replicates was used, and the adsorption was optimised using response surface methodology, considering the amount of activated carbon (X_1) and agitation time (X_2) as variables, as shown in Table 2.

Table 2. Factors, codes, and values determined in the adsorption of metals from water samples with activated carbon

Factors	Unit	Code	-1	0	+1
Amount of activated carbon	g	X_1	1	3	5
Stirring time	min	X_2	30	60	90

Statistical analysis of the generated data was performed using the Statgraphics CENTURION XIX software, version 19.1.2 (StatPoint, 2020).

The response variables ($Y_{Fe,\ Al,\ Cu,\ Zn}$), show the adsorption of the metals (Eq. 2).

$$Y_{Fe,Al,Cu,Zn} = B_0 + B_1X_1 + B_2X_2 + B_{11}X_1^2 + B_{12}X_1X_2 + B_{22}X_2^2 \quad (2)$$

where $Y_{Fe,Al,Cu,Zn}$ – response variable (adsorption of Fe^{+2}, Al^{+3}, Cu^{+2}, Al^{+2}); B_0 – coefficient of the constant; B_1 and B_2 – linear coefficients; B_{12} – binary interaction coefficient; B_{11} and B_{22} – quadratic coefficients, and X_1 and X_2 – coded values of the variables responsible for the adsorbed metal.

RESULTS AND DISCUSSION

Characterization of the raw material, production of activated carbon, pyrolysis, and ANOVA

The analysis of variance (ANOVA) of the data obtained for the amount of activated carbon as a function of the modification temperature, activation time, and pyrolysis and activation temperatures is reported in Table 3.

The statistical significance was observed in factors C and B^2 ($p \leq 0.05$), which corresponds to the activation time and the quadratic effect of the pyrolysis and activation temperature.

Table 3. ANOVA for the fitted quadratic polynomial model for activated carbon manufacture

Source of variation	Sum of squares	gl	Mean square	*F*-ratio	*P*-value
A: Modification temperature	0.1701	1	0.1701	0.05	0.8257^{ns}
B: Pyrolysis/activation temperature	5.4891	1	5.4891	1.61	0.2212^{ns}
C: Activation time	85.4996	1	85.4996	25.12	0.0001*
A^2	2.4876	1	2.4876	0.73	0.4045^{ns}
AB	2.1168	1	2.1168	0.62	0.4412^{ns}
AC	1.2936	1	1.2936	0.38	0.5457^{ns}
B^2	62.1675	1	62.1675	18.27	0.0005*
BC	0.3571	1	0.3571	0.10	0.7500^{ns}
C^2	0.2576	1	0.2576	0.08	0.7865^{ns}
Error	57.8564	17	3.4033		
CV (%)	16.7000				
R^2	0.7342				

ns and *, not significant and significant, respectively, $p \leq 0.05$ using the *F* test; CV: coefficient of variation; R^2: coefficient of determination.

After optimising the variables used in the production of activated carbon, 18.41 g was determined as the optimum quantity, obtained at 100 °C modification temperature, 400 °C pyrolysis and activation temperature, and 1 h of activation time. Eq. 3 shows the optimal variables generated by the software:

$$\hat{y}_1 = 115.74 - 10.5406^{*}X_3 + 0.00032189^{*}X_2^2 \quad (3)$$

The graph of the optimisation of obtaining activated carbon from cocoa pod husks (in g) is shown in Fig. 1, A, which corresponds to the response surface, while Fig. 1, B shows the analysis of the main effects. At lower modification and pyrolysis temperatures, there was a higher yield of activated carbon. The activation time had a negative effect because increasing its value decreased the production of activated carbon.

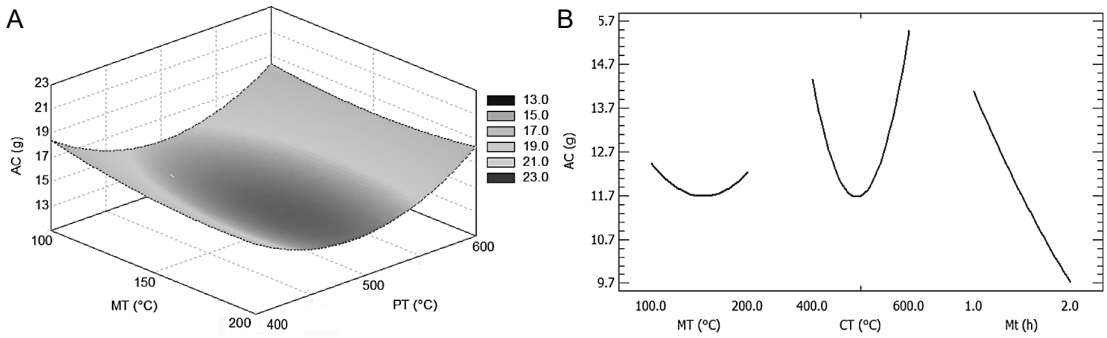

Figure 1. Effect of modification temperature, pyrolysis and activation temperature (A), and activation time (B) on obtaining activated carbon from cocoa pod husks.

MT – Modification Temperature; PT – Pyrolysis and Activation Temperature; AC – Activated Carbon; Mt – Modification Time.

Using lignocellulose materials from forestry and food industries as raw materials to manufacture activated carbon using pyrolysis, to be used as an adsorbent (Martelo et al., 2022), reduces costs, revaluates and minimises industrial waste, and becomes a viable alternative for carbon capture, thereby optimising environmental management and taking advantage of the benefits of its chemical composition.

Cocoa pods, depending on the variety, and according to Díaz-Oviedo et al. (2022) and Lara et al. (2016), have 43.6 and 12.66% lignin, 34.4 and 19.82% cellulose, and 11.75 and 9.45% hemicellulose, respectively, the latter two being carbohydrates, which decompose independently during pyrolysis (Kim et al., 2022), because hemicellulose is the first component to degrade between 220 and 315 °C (Yang et al., 2007). In contrast, at temperatures between 300 and 400 °C, cellulose undergoes decarbonisation, ring-opening polymerisation, and aromatisation (Hoang et al., 2021) to form aromatic groups (Lara et al., 2016). According to Ma et al. (2016), the pyrolysis of lignin leads to the transformation of methoxyl groups (-O-CH_3), and total phenol groups and G-type phenols (guaiacol) increase at 500 °C; however, from 400 to 700 °C, S-type phenols (syringol) decrease, while P-type phenols (phenol) and C-type phenols (catechol) increase, which are important for giving activated carbon its adsorbent characteristics.

Rincón et al. (2015) reported that the production of activated carbon typically involves two stages: the carbonisation (pyrolysis) of the raw material, and the activation of the carbonised material at temperatures of ≥ 500 °C. In the current study, it was carbonised and activated at 400, 500, and 600 °C. The high carbonisation and activation temperatures (700 °C) give the activated carbon larger pores (mesopores), making it suitable for water treatment (Rincón et al., 2015). Wang et al. (2021) stated that the production of activated carbon from lignocellulosic biomass comprises two main processes, activation and pyrolysis, which were applied in this study.

In the production of activated carbon, the pyrolysis temperature a considerable influence on its texture, which in turn influences its adsorbent properties depending on its pore type. Rodríguez-Sánchez et al. (2019), when processing chestnut (*Castanea sativa Mill*) waste activated carbon at low-temperature (220 °C) carbonisation, obtained BET areas (specific surface areas) of 3 m^2 g^{-1}, whereas at 800 °C, the BET area was 568 m^2 g^{-1}, and the micropore and mesopore volumes were 0.133 cm^3 g^{-1} and 0.033 cm^3 g^{-1}, respectively. Notably, the temperature, residence time, and heating rate have a substantial impact on pyrolysis (Yogalakshmi et al., 2022).

In this regard, Chen et al. (2022) indicated that during pyrolysis, lignocellulosic components were degraded, generating the first volatile hemicellulose compounds, followed by cellulose, and then volatile lignin.

The pyrolysis of lignocellulose feedstocks leads to the formation of carbon, depolymerisation, and fragmentation of molecules via various mechanisms. In this regard, Chen et al. (2022) indicated that during pyrolysis, lignocellulosic components were degraded, generating the first volatile hemicellulose compounds, followed by cellulose, and then volatile lignin. Pyrolysis of lignin generates hydrocarbons due to aromatic rings and methoxy groups. With increasing temperature, the carboxy-C and O-alkyl-C structures in biochar decrease, whereas aryl-C increases due to deoxygenation reactions such as dehydroxylation, decarboxylation, decarbonylation, and demethoxylation, which reduce the amount of oxygen-containing functional groups (such as -OH, -C=O, -COOH, and -OCH_3), and polycondensation reactions, leading to the formation of more polycyclic aromatic hydrocarbon units during pyrolysis. According to Nyirenda et al. (2022), the heat treatment produced by pyrolysis develops oxide compounds on the surface of activated carbon, which directly influences its ability to remove metals from water samples.

Adsorbent activity, metal adsorption mechanisms of activated carbon, and ANOVA

The results of the statistical analysis of the data generated by the adsorptive action of the activated in removing Fe^{2+}, Al^{3+}, Cu^{2+}, and Zn^{2+} as water pollutants, as well as their significance, are presented in Table 4.

Table 4. Summary of removal of Fe^{+2}, Al^{+3}, Cu^{+2}, and Zn^{+2} according to ANOVA

Sources of variation	*P*-value			
	Fe^{2+}	Al^{3+}	Cu^{2+}	Zn^{2+}
A: Amount of activated carbon	0.0000*	0.0000*	0.0000*	0.0000*
B: Stirring time	0.0000*	0.0001*	0.0000*	0.0000*
AA	0.0002*	0.0000*	0.2014^{ns}	0.6955^{ns}
AB	0.0000*	0.0048*	0.0020*	0.5082^{ns}
BB	0.9912^{ns}	0.0001*	0.6326^{ns}	0.8754^{ns}
CV (%)	37.52	36.95	32.28	38.34

ns and *, not significant and significant, respectively, $p \leq 0.05$ using the *F* test; CV: coefficient of variation.

A 5% significance level was set for the removal of Fe^{2+}, Al^{3+}, Cu^{2+}, and Zn^{2+} as the amount of activated carbon used correlated with the stirring time at $p \leq 0.05$. Table 5 lists the adjusted metal removal models.

Table 5. Coefficient of determination and fitted models of metal removal

Metal removed	R^2	Adjusted R^2	Equation	
Fe^{2+}	0.9787	0.9711	$\hat{y}_{Fe^{2+}} = 1.06911 - 0.090333^{*}X_1 - 0.0067889^{*}X_2 - 0.002425^{*}X_1X_2 - 0.000167^{*}X_1^2$	(4)
Al^{3+}	0.9937	0.9913	$\hat{y}_{Al^{3+}} = 0.1560 - 0.035^{*}X_1 + 0.002478^{*}X_2 - 0.0001417^{*}X_1X_2 + 0.0095^{*}X_1^2 - 0.0000339^{*}X_2^2$	(5)
Cu^{2+}	0.9224	0.8938	$\hat{y}_{Cu^{2+}} = 0.033889 + 0.001733^{*}X_1 - 0.000233^{*}X_2 - 0.00008417^{*}X_1X_2$	(6)
Zn^{2+}	0.9266	0.8996	$\hat{y}_{Zn^{2+}} = 0.0084556 - 0.0007333^{*}X_1 - 0.00005389^{*}X_2$	(7)

* denotes significance at $p \leq 0.05$ using the *F* test; R^2: coefficient of determination.

It is considered that there was a good fit in the models because the coefficients of determination (R^2), including the adjusted R^2, ranged from 0.9224 to 0.9937 and 0.8938 to 0.9913, respectively (Table 5), in all the tests performed at the laboratory level, owing to the type of experimental design, which allowed us to determine the influence of the independent variables on the removal of metals from the water samples of the Ucayali River (Fig. 2).

The optimum removal value, according to the fitted model, was 0.778 ppm for Fe^{2+}, with 1.0 g of activated carbon and a stirring time of 90.0 min (Eq. 4); 0.171 ppm for Al^{3+}, with 1.0 g of activated carbon and a stirring time of 34.5 min (Eq. 5); 0.027 ppm for Cu^{2+}, with 1.0 g of activated carbon and a stirring time of 30.0 min (Eq. 6);

and 0.0061 ppm for Zn^{2+}, with 1.0 g of activated carbon and a stirring time of 30.0 min (Eq. 6; Fig. 2).

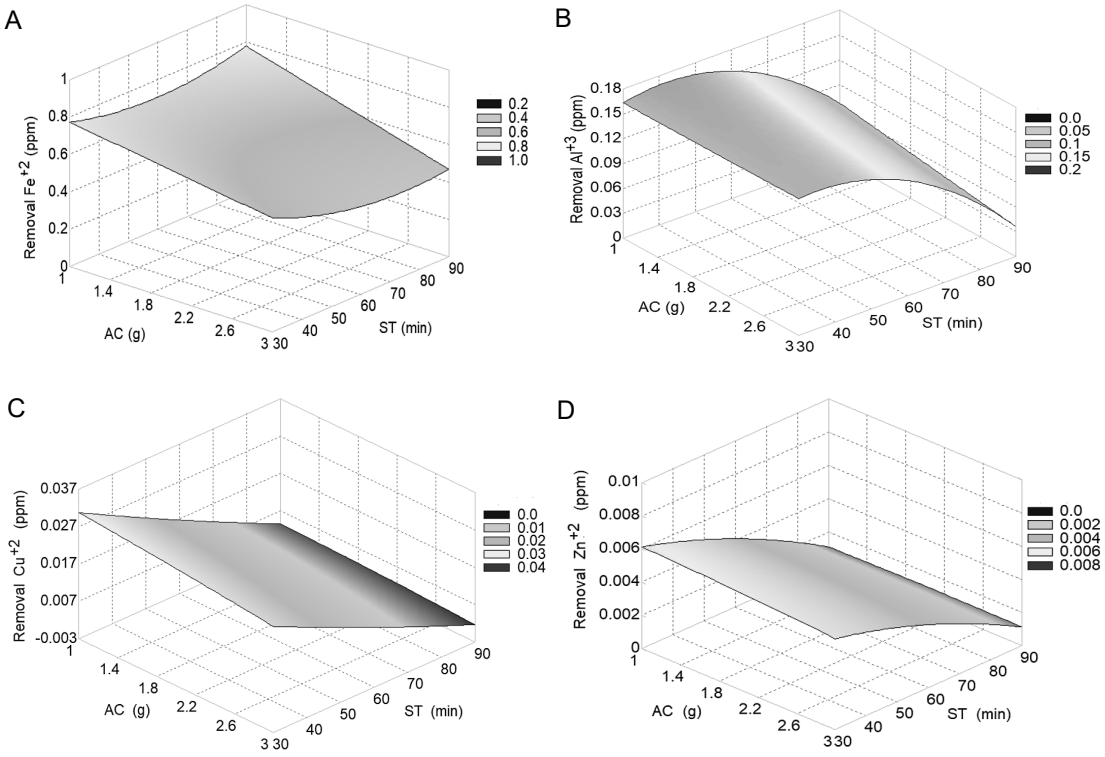

Figure 2. Effect of the amount of activated carbon and the agitation time on the removal of Fe^{2+}, Al^{3+}, Cu^{2+}, and Zn^{2+} from water samples from the Ucayali River, Peru.
ST – Stirring Time; AC – Activated Carbon.

The adsorptive effect of activated carbon on the removal of metals from water samples from the Ucayali River was obtained from the optimization of the models, which were developed under ideal conditions, and 1 g of activated carbon was established as the effective amount to remove Fe^{2+}, Al^{3+}, Cu^{2+}, y, and Zn^{2+} (Table 6).

Table 6. Percentage of metals removed from water samples with 1 g of activated carbon from cocoa pod shells

	Metal concentration (ppm)			
	Fe^{2+}	Al^{3+}	Cu^{2+}	Al^{2+}
Initial content	1.370	0.250	0.041	0.0110
Amount adsorbed	0.778	0.171	0.027	0.0061
% removed	56.8	68.4	65.9	55.5

The adsorptive effectiveness of activated carbon depends on the carbonisation temperature and the activation method. Narvekar et al. (2021) obtained activated carbon with a pore volume of 0.08 $m^3\ g^{-1}$ and a surface area of 425 $m^2\ g^{-1}$ at 800 °C in the presence of N_2. These are fundamental factors to guarantee the adsorptive power of biochar, whose functionality is provided by C=C bonds (alkene group) and the -SO_3H group (sulphone). The sulfone group has surfactant properties and is used for the removal of metals from wastewater by chemisorption, for example, of Cd^{2+} and Pb^{2+} (Gul et al., 2022).

Ahmad et al. (2018) manufactured activated carbon from banana peels (*Musa paradisiaca*) and cauliflower leaves (*Brassica oleracea* var. botrytis) by thermal modification in an oven at 200 °C for 1 h, then by pyrolysis and activation at 600 °C for 2 h. Subsequently, they were crushed to particles of 0. 452–1 mm, with which they removed metals from water by adsorption. The banana peels had the highest adsorption efficiency, being in the order of removal of $Pb^{2+} > Cu^{2+} > Cd^{2+}$, with the electrostatic attraction being the predominant mechanism governing the sorption process.

Lara et al. (2016) used washed, dehydrated, and ground cocoa shells as a bioadsorbent to remove Pb^{2+} (91.32%) and Cd^{2+} (87.80%) from wastewater samples, attributing the bioadsorption to the action of aromatic groups, specifically C-H and C=C.

Valdés-Rodríguez et al. (2022) obtained activated carbon from jacaranda (*Jacaranda mimosifolia*) and guava (*Psidium guajava*) seed residues and grape pomace (*Vitis vinifera*) and sugar cane bagasse (*Saccharum officinarum*), resulting in the jacaranda seed biochar being the most efficient for adsorbing Hg^{2+} and Pb^{2+} from wastewater samples at pyrolysis at 800 °C for 4 h, attributing the adsorption mechanism to the oxygenated functional groups present in the activated carbon.

Namasivayam et al. (2007) used activated carbon from pine nut (*Jatropha curcas*) shells, pyrolysed at 700 °C in a muffle furnace for 1 h, with particles of 250–500 μ, and successfully removed Cr^{6+}, V^{5+}, and Ni^{2+} from water samples, attributing the adsorption capacity to its large surface area, its microporous characteristic, and the chemical nature of its surface.

Using plant-derived activated carbon with additives to improve adsorption capacity has been demonstrated by Nyirenda et al. (2022), who employed a silver-silica nanocomposite using activated carbon as a support, with which they were able to adsorb 84.75, 81.30, 87.72, and 81.97 mg g^{-1} for Cu^{2+}, Pb^{2+}, Cd^{2+}, and Zn^{2+}, respectively. The removal of these metals by activated carbon adsorption occurs via electrostatic interactions between the dissolved cations and negatively charged silanolate surface sites; however, ion exchange is the main adsorption mechanism (Ahmad et al., 2017).

New alternatives to improve the adsorption capacity of activated carbon from cellulose are being experimented to maximise its capacity to remove metals present in water. Mubarak et al. (2022) experimented with activated carbon and a nanocomposite of carborundum and microcrystalline cellulose, which acted as an exceptional active adsorbent for the adsorption of As^{3+} and Cu^{2+} ions for water treatment. The main mechanism of adsorption of the ions by the nanocomposite was electrostatic interaction at moderate pH values (above 6), while at high acidity conditions (pH 2–6), the dominant mechanism was chemical complexation.

CONCLUSION

The production of activated carbon from cocoa pod husks by pyrolysis can be applied to various lignocellulose raw materials because the activation and modification of cellulose, hemicellulose, and lignin provides a large surface area, suitable surface functional groups, and appropriate pore diameters that confer adsorbent potential. The adsorption and heavy metal removal efficiencies of the activated carbon was a function of the parameters used for its production, such as a modified temperature of 100 °C, activation time of 1 h, and pyrolysis and activation temperatures of 400 °C, with which 18.41 g of activated carbon was obtained from cocoa husks. Moreover, 56.8%, 68.4%,

65.9%, and 55.5% of iron, aluminium, copper, and zinc was removed, verifying its use in the manufacture of filters to decontaminate water with heavy metals.

REFERENCES

Adeyeye, S.A.O. & Ashaolu, T.J. 2020. A Study on Polycyclic Aromatic Hydrocarbon and Heavy Metal Concentrations of Commercial Grilled Meat (Suya) and Smoked Catfish (Clarias gariepinus Burchell, 1822) Fish from South-West, Nigeria. *Polycyclic Aromatic Compounds* **42**(6), 3281–3290. doi:10.1080/10406638.2020.1858883

Ahmad, I., Siddiqi, W.A. & Ahmad, T. 2017. Synthesis, Characterization of Silica Nanoparticles and Adsorption Removal of Cu 2+ Ions in Aqueous Solution. *International Journal of Emerging Technology and Advanced Engineering* **7**(8), 439–445.

Ahmad, Z., Gao, B., Mosa, A., Yu, H., Yin, X., Bashir, A., Ghoveisi, H. & Wang, S. 2018. Removal of Cu(II), Cd(II) and Pb(II) ions from aqueous solutions by biochars derived from potassium-rich biomass. *Journal of Cleaner Production* **180**, 437–449. doi:10.1016/j.jclepro.2018.01.133

Akila, M., Anbalagan, S., Lakshmisri, N., Janaki, V., Ramesh, T., Merlin, R.J. & Kamala-Kannan, S. 2022. Heavy metal accumulation in selected fish species from Pulicat Lake, India, and health risk assessment. *Environmental Technology and Innovation* **27**, 102744. doi:10.1016/j.eti.2022.102744

Aksoy, D. & Ercan Sagol. 2016. Application of central composite design method to coal flotation: Modelling, optimization and verification. *Fuel* **183**, 609–616. doi:10.1016/j.fuel.2016.06.111

ASTM. 1997. Standard test method for determination of moisture content of particulate wood fuels using a microwave oven E 1358–97 (Reapproved 2006). *ASTM International* **11**(10), 1–2. doi:10.1520/E1358 -97R13.2

Baby, R. & Hussein, M.Z. 2020. Ecofriendly Approach for Treatment of Heavy-Metal-Contaminated Water Using Activated Carbon of Kernel Shell of Oil Palm. *Materials* **13**(11), 2627. doi:10.3390/ma13112627

Ccanccapa-Cartagena, A., Paredes, B., Vera, C., Chavez-Gonzales, F.D., Olson, E., Welp, L.R. & Jafvert, C.T. 2021. Occurrence and probabilistic health risk assessment (PRA) of dissolved metals in surface water sources in Southern Peru. *Environmental Advances* **5**, 100102–100102. doi:10.1016/j.envadv.2021.100102

Chen, D., Cen, K., Zhuang, X., Gan, Z., Zhou, J., Zhang, Y. & Zhang, H. 2022. Insight into biomass pyrolysis mechanism based on cellulose, hemicellulose, and lignin: Evolution of volatiles and kinetics, elucidation of reaction pathways, and characterization of gas, biochar and bio-oil. *Combustion and Flame* **242**, 112142–112142. doi:10.1016/j.combustflame.2022.112142

Chen, D., Xie, S., Chen, C., Quan, H., Hua, L., Luo, X. & Guo, L. 2017. Activated biochar derived from pomelo peel as a high-capacity sorbent for removal of carbamazepine from aqueous solution. *RSC Advances* **7**(87), 54969–54979. doi:10.1039/c7ra10805b

Choi, Y. & Kan, E. 2019. Effects of pyrolysis temperature on the physicochemical properties of alfalfa-derived biochar for the adsorption of bisphenol A and sulfamethoxazole in water. *Chemosphere* **218**, 741–748. doi:10.1016/j.chemosphere.2018.11.151

Cruz, G.L., Pirilä, M., Huuhtanen, M., Carrión, L., Alvarenga, E. & Keiski, R.L. 2012. Production of Activated Carbon from Cocoa (Theobroma cacao) Pod Husk. *Journal of civil & environmental engineering* **2**(2). doi:10.4172/2165-784x.1000109

Díaz-Oviedo, A.F, Ramón-Valencia, B.A. & Moreno-Contreras, G. 2022 Physical- chemical characterization of the cocoa pod husk as a possible use in the production of agglomerated boards. *Revista de Investigación, Desarrollo e Innovación* **12**(1), 97–106 (in Spanish). doi:10.19053/20278306.v12.n1.2022.14211

Fathy, M., Zayed, A.I. & Ahmed, H.B. 2022. Activated Carbon/Carborundum@Microcrystalline Cellulose core shell nano-composite: Synthesis, characterization and application for heavy metals adsorption from aqueous solutions. *Industrial Crops and Products* **182**, 114896. doi:10.1016/j.indcrop.2022.114896

González-García, P., Centeno, T.A., Urones-Garrote, E., Ávila-Brande, D. & Otero-Díaz, L. 2013. Microstructure and surface properties of lignocellulosic-based activated carbons. *Applied Surface Science* **265**, 731–737. doi:10.1016/j.apsusc.2012.11.092

Grich, A., Taoufiq Bouzid, T., Aicha Naboulsi, Abdelmajid Regti, Abdelaaziz Aloui Tahiri, Mamoune El Himri, & Mohammadine El Haddad. 2024. Preparation of low-cost activated carbon from Doum fiber (Chamaerops humilis) for the removal of methylene blue: Optimization process by DOE/FFD design, characterization, and mechanism. *Journal of Molecular Structure* **1295**, 136534–136534. doi:10.1016/j.molstruc.2023.136534

Gul, S., Ahmad, Z., Asma, M., Ahmad, M., Rehan, K., Munir, M., Bazmi, A.A., Ali, H.M., Mazroua, Y., Salem, M.L., Akhtar, M., Khan, M.S., Chuah, L.F. & Asif, S. 2022. Effective adsorption of cadmium and lead using SO3H-functionalized Zr-MOFs in aqueous medium. *Chemosphere* **307**, 135633. doi:10.1016/j.chemosphere.2022.135633

Guo, X., Dong, H., Yang, C., Zhang, Q., Liao, C., Zha, F. & Gao, L. 2016. Application of goethite modified biochar for tylosin removal from aqueous solution. *Colloids and Surfaces A: Physicochemical and Engineering Aspects* **502**, 81–88. doi:10.1016/j.colsurfa.2016.05.015

Hoang, A.T., Show, P.L., Fattah, I.R., Chong, C.T., Cheng, C.K., Sakthivel, R. & Kim, K. 2021. Progress on the lignocellulosic biomass pyrolysis for biofuel production toward environmental sustainability. *Fuel Processing Technology* **223**, 106997. doi:10.1016/j.fuproc.2021.106997

Kim, H., Yu, S., Kim, M. & Ryu, C. 2022. Progressive deconvolution of biomass thermogram to derive lignocellulosic composition and pyrolysis kinetics for parallel reaction model. *Energy* **254**, 124446. doi:10.1016/j.energy.2022.124446

Lara, J., Tejada, C., Villabona, A. & Arrieta, A. 2016. Adsorption of lead and cadmium in continuous of fixed bed on cocoa waste. *Revista Ion* **29**(2), 111–122 (in Spanish). doi:10.18273/revion.v29n2-2016009

Liu, Z., Sun, Y., Xu, X., Qu, J. & Qu, B. 2020. Adsorption of Hg(II) in an Aqueous Solution by Activated Carbon Prepared from Rice Husk Using KOH Activation. *ACS omega* **5**(45), 29231–29242. doi:10.1021/acsomega.0c03992

López, M. & Alva, F. 2022. UCAYALI: Síntesis de Actividad Económica FEBRERO 2022. Banco Central de Reserva del Perú. Departamento de Estudios Económicos, Iquitos, Perú (in Spanish). https://www.bcrp.gob.pe/docs/Sucursales/Iquitos/2022/sintesis-ucayali-02-2022.pdf. Accessed 12.09.2023

Ma, Z., Sun, Q., Ye, J., Yao, Q. & Zhao, C. 2016. Study on the thermal degradation behaviors and kinetics of alkali lignin for production of phenolic-rich bio-oil using TGA–FTIR and Py–GC/MS. *Journal of Analytical and Applied Pyrolysis* **117**, 116–124. doi:10.1016/j.jaap.2015.12.007

Mariana, M., Khalil, H.P.S.A., Mistar, E.M., Yahya, E.B., Alfatah, T., Danish, M. & Amayreh, M.Y. 2021. Recent advances in activated carbon modification techniques for enhanced heavy metal adsorption. *Journal of water process engineering* **43**, 102221. doi:10.1016/j.jwpe.2021.102221

Martelo, N., Antxustegi, M., Corro, E., Baloch, M., Volpe, R., Gagliano, A., Fichera, A. & Alriols, M.G. 2022. Use of residual lignocellulosic biomass for energetic uses and environmental remediation through pyrolysis. *Energy Storage and Saving* **1**(3), 129–135. doi:10.1016/j.enss.2022.04.004

Maulina, S. & Iriansyah, M. 2018. Characteristics of activated carbon resulted from pyrolysis of the oil palm fronds powder. *IOP Conference Series: Materials Science and Engineering* **309**, 012072. doi:10.1088/1757-899x/309/1/012072

Mubarak, M.F., Zayed, A.M. & Ahmed, H.A. 2022. Activated Carbon/Carborundum@Microcrystalline Cellulose core shell nano-composite: Synthesis, characterization and application for heavy metals adsorption from aqueous solutions. *Industrial Crops and Products* **182**, 114896–114896. doi:10.1016/j.indcrop.2022.114896

Namasivayam, C., Sangeetha, D. & Gunasekaran, R. 2007. Removal of Anions, Heavy Metals, Organics and Dyes from Water by Adsorption onto a New Activated Carbon from Jatropha Husk, an Agro-Industrial Solid Waste. *Chemical Engineering Research and Design* **85**(2), 181–184. doi:10.1205/psep05002

Nandeshwar, S.N., Mahakalakar, A.S., Gupta, R. & Kyzas, G.Z. 2016. Green activated carbons from different waste materials for the removal of iron from real wastewater samples of Nag River, India. *Journal of Molecular Liquids* **216**, 688–692. doi:10.1016/j.molliq.2015.12.065

Narvekar, A.A., Fernandes, J.O., Naik, S.N. & Tilve, S.G. 2021. Development of glycerol based carbon having enhanced surface area and capacitance obtained by KOH induced thermochemical activation. *Materials Chemistry and Physics* **261**, 124238. doi:10.1016/j.matchemphys.2021.124238

Nyirenda, J., Kalaba, G.M. & Munyati, O. 2022. Synthesis and characterization of an activated carbon-supported silver-silica nanocomposite for adsorption of heavy metal ions from water. *Results in engineering* **15**, 100553. doi:10.1016/j.rineng.2022.100553

Odubiyi, O.A., Awoyale, A.A. & Eloka-Eboka, A.C. 2012. Wastewater Treatment with Activated Charcoal Produced from Cocoa Pod Husk. *International Journal of Environment and Bioenergy* **4**(3), 162–175.

Olaoye, R.A., Afolayan, O.D., Mustapha, O.I. & Adeleke, H.O. 2018. The Efficacy of Banana Peel Activated Carbon in the Removal of Cyanide and Selected Metals from Cassava Processing Wastewater. *Advances in research* **16**(1), 1–12. doi:10.9734/air/2018/43070

Prastuti, O.P., Septiani, E., Kurniati, Y., Widiyastuti, P. & Setyawan, H. 2019. Banana Peel Activated Carbon in Removal of Dyes and Metals Ion in Textile Industrial Waste. *Materials Science Forum* **966**, 204–209. doi:10.4028/www.scientific.net/msf.966.204

Rincón, J.S., Rincón, S., Guevara, P., Ballén, D.A.S., Morales, J.C. & Monroy, N. 2015. Production of activated carbon by physical methods from El Cerrejon coal and its application in the treatment of wastewater from dyeing plants. *Revista de la Academia Colombiana de Ciencias Exactas, Físicas y Naturales* **39**(51), 171–175 (in Spanish). doi:10.18257/raccefyn.138

Rodríguez-Sánchez, S., Ruiz, B.A., Martínez-Blanco, D., Sánchez-Arenillas, M., Diez, M.A., Suárez-Ruiz, I., Marco, J.F., Blanco, J.E. & Fuente, E. 2019. Sustainable Thermochemical Single-Step Process To Obtain Magnetic Activated Carbons from Chestnut Industrial Wastes. *ACS Sustainable Chemistry & Engineering* **7**(20), 17293–17305. doi:10.1021/acssuschemeng.9b04141

Sabela, M.I., Kunene, K., Kanchi, S., Xhakaza, N.M., Bathinapatla, A., Mdluli, P.S., Sharma, D. & Bisetty, K. 2019. Removal of copper (II) from wastewater using green vegetable waste derived activated carbon: An approach to equilibrium and kinetic study. *Arabian Journal of Chemistry* **12**(8), 4331–4339. doi:10.1016/j.arabjc.2016.06.001

Sadheesh, S., Shankar, R., Kumar, S. & Prasath, B.G. 2021. Contaminated water treatment with Activated charcoal build from cocoa pod husk. *IOP conference series* **1145**(1), 012027. doi:10.1088/1757-899x/1145/1/012027

Sibal, L.N. & Espino, M.P.B. 2018. Heavy metals in lake water: a review on occurrence and analytical determination. *International Journal of Environmental Analytical Chemistry* **98**(6), 536–554. doi:10.1080/03067319.2018.1481212

Solanki, A. & Boyer, T.H. 2017. Pharmaceutical removal in synthetic human urine using biochar. *Environmental science* **3**(3), 553–565. doi:10.1039/c6ew00224b

Tsai, C., Tsai, W., Liu, S. & Lin, Y. 2018. Thermochemical characterization of biochar from cocoa pod husk prepared at low pyrolysis temperature. *Biomass Conversion and Biorefinery* **8**(2), 237–243. doi:10.1007/s13399-017-0259-5

Valdés-Rodríguez, E., Mendoza-Castillo, D.I., Reynel-Avila, H.E., Aguayo-Villarreal, I.A. & Bonilla-Petriciolet, A. 2022. Activated carbon manufacturing via alternative Mexican lignocellulosic biomass and their application in water treatment: Preparation conditions, surface chemistry analysis and heavy metal adsorption properties. *Chemical engineering research and design* **187**, 9–26. doi:10.1016/j.cherd.2022.08.039

Wang, H., Chen, D., Huang, L., Zhang, Y., Zhang, Y., Wang, A., Xiao, G., Zhang, W., Lei, H. & Ruan, R. 2021. Activated carbon from lignocellulosic biomass as catalyst: A review of the applications in fast pyrolysis process. *Journal of Analytical and Applied Pyrolysis* **158**, 105246. doi:10.1016/j.jaap.2021.105246

Wu, L., Yang, N., Li, B. & Bi, E. 2018. Roles of hydrophobic and hydrophilic fractions of dissolved organic matter in sorption of ketoprofen to biochars. *Environmental Science and Pollution Research* **25**(31), 31486–31496. doi:10.1007/s11356-018-3071-2

Yang, H., Yan, R., Chen, H., Lee, D.H. & Zheng, C. 2007. Characteristics of hemicellulose, cellulose and lignin pyrolysis. *Fuel* **86**(12–13), 1781–1788. doi:10.1016/j.fuel.2006.12.013

Yogalakshmi, K.,T, Sivashanmugam, P.D., Kavitha, S., Kannah, R.Y., Varjani, S., Adishkumar, S., Aslam, M. & Rajesh, B.J. 2022. Lignocellulosic biomass-based pyrolysis: A comprehensive review. *Chemosphere* **286**, 131824. doi:10.1016/j.chemosphere.2021.131824

Yunus, Z.M., Al-Gheethi, A., Othman, N., Hamdan, R. & Ruslan, N.N. 2020. Removal of heavy metals from mining effluents in tile and electroplating industries using honeydew peel activated carbon: A microstructure and techno-economic analysis. *Journal of Cleaner Production* **251**, 119738. doi:10.1016/j.jclepro.2019.119738

Zaghloul, G., El-Din, H.M.S., Mohamedein, L.I. & El-Moselhy, K.M. 2022. Bio-accumulation and health risk assessment of heavy metals in different edible fish species from Hurghada City, Red Sea, Egypt. *Environmental Toxicology and Pharmacology* **95**, 103969. doi:10.1016/j.etap.2022.103969